Accepted by Ultramicroscopy: https://doi.org/10.1016/j.ultramic.2020.113163

FANM: A software for focus and aberrations of nuclear microprobe

Yanxin Dou*, Jeroen Anton van Kan
Center for Ion Beam Applications, Department of Physics, National University of Singapore, 2 Science Drive 3, Singapore 117542, Singapore

*Corresponding author
Email address: douyanxinch@163.com

Abstract

Focus and Aberrations of Nuclear Microprobe (FANM) is a new beam optics package to achieve fast and accurate design of a nuclear microprobe. FANM achieves a balance between speed of focusing and accuracy of high order aberrations. A combined method proposed in FANM is to achieve focusing conditions using a matrix method and to calculate aberration coefficients using a numerical ray tracing method. FANM has two optional optimization algorithms (derivative-free method and particle swarm optimization), offering a powerful choice for multi-variable optimization. Numeric variables in FANM are stored as 64-bit (8-byte) double-precision floating-point values to reduce calculation errors. Results obtained with FANM are compared with six existing computational tools (PRAM, TRANSPORT-PSI, TRANSPORT-PBO, WinTRAX, GEANT4-nanobeam and Zgoubi). The reasons for discrepancies between the different packages are discussed. Calculated currents of magnetic quadrupole lenses obtained with FANM are compared with experimental values of a nuclear microprobe in the National University of Singapore.

Keywords: nuclear microprobe; beam optics; aberration; software.

1. Introduction

Fundamentals of ion-material interactions have been widely studied, the detailed insight of these interactions has spurred the development of ion beam analysis (IBA) [1-3], ion beam modification of materials (IBMM) [4-6], ion beam fabrication (IBF) [7-10] and ion beam irradiation (IBI) [11-13]. Nuclear microprobe, with an advantage of focusing ions into micron or sub-micron diameter in a plane, provides a unique method in those fields. On the website of IAEA [14], the number of nuclear microprobes listed is more than 150. Most of them are equipped with a focusing lens system from the OXFORD MICROBEAMS or Microanalytical Research Centre Commercial Organisation (MARCO, University of Melbourne), adopting a layout of (spaced) Oxford triplet or (spaced) Russian quadruplet

[15][16]. Major challenges of a high resolution nuclear microprobe are the brightness of an accelerator and the acceptance of a focusing lens system [17]. Other challenges, such as parasitic aberrations, may dominate the final performance of a lens system. However, the discussion of parasitic aberrations is excluded in this paper since they can be essentially eliminated with modern manufacturing methods [17]. Efforts to improve the brightness can be found in literatures [18-22]. A large acceptance means a high ion utilization efficiency in a nuclear microprobe. Acceptance of a focusing lens system is normally determined by the demagnification, spherical aberration and chromatic aberration [17]. When spherical aberration is the dominant aberration, ignoring chromatic aberration and the spherical aberration cross-terms, a figure of merit defined by Ryan and Jamieson can be simply used as a good indicator to system performance [23]. To achieve a larger acceptance the current beam optics designs for nuclear microprobes have to be improved.

For many years, two methods have been used to calculate the imaging properties of a focusing lens system: matrix methods and numerical ray tracing methods. Matrix methods have the advantage of simplicity and speed of calculation, while their accuracy and usefulness are normally limited [15]. Numerical ray tracing methods have the advantage of accuracy and less assumptions, while they are normally time consuming to achieve focusing conditions [16]. In order to achieve a balance between speed and accuracy, a new approach is presented here. The new approach, which is adopted in Focus and Aberrations of Nuclear Microprobe (FANM), is to achieve focusing conditions using a matrix method and then calculate aberration coefficients using a numerical ray tracing method. Meanwhile, FANM offers two optional optimization algorithms (derivative-free method and particle swarm optimization) to enhance its searching ability.

The FANM standalone executable file is available for free on a website (https://github.com/CHNDOU/FANM). A brief tutorial is provided in the "README.txt" file. In future, updated versions of FANM will also be uploaded to this website.

Principles of FANM are explained in details in section 2. Using the layout of the second generation proton beam writing beamline in Singapore [24][25], comparisons of FANM with six other beam optics software packages (PRAM, TRANSPORT-PSI, TRANSPORT-PBO, WinTRAX, GEANT4-nanobeam and Zgoubi) are presented in section 3. Ideal currents required for beam focusing in magnetic quadrupole lenses obtained via FANM are compared with experimental values in section 4.

2. Principles of FANM

Equations of motion of an ion in magnetic and electrostatic fields can be found in [15]. In the case of a nuclear microprobe, static magnetic quadrupole lenses are presently the most extensive use to focus fast ions. Therefore, the following equation is used in FANM to describe the motion of a fast ion in static magnetic fields:

$$\frac{d\boldsymbol{p}}{dt} = qe(\boldsymbol{v} \times \boldsymbol{B}) \tag{1}$$

Where $\boldsymbol{p}$ and qe is the momentum and charge of the ion, q is its charge number, e is elementary electric charge, $\boldsymbol{v}$ is its velocity and $\boldsymbol{B}$ is the magnetic field. In a magnetic

field, the energy of an ion does not change, so the characteristics of the motion of the ion are determined only by its momentum, charge and the distribution of the magnetic field. The momentum and charge of an ion in equation (1) can be instead by magnetic rigidity, which is defined as $B\rho = p/(qe)$. For a given distribution of magnetic fields and magnetic rigidity of an ion, the motion characteristics of the ion are determined. Then coordinates of the ion in the magnetic fields can be derived from initial coordinates of the ion.

To solve motion characteristics of an ion in a given distribution of magnetic fields, there are two methods: matrix method and numerical ray tracing method. A detailed description of the matrix method and numerical ray tracing method can be found in [15] and [16]. The matrix method is simple and fast in first order, but it is relatively complicated in the third and higher order. In contrast, the numerical ray tracing method directly trace special rays in any distribution magnetic field. It has a natural advantage of calculating arbitrary order aberrations by changing the number of rays traced through the fields, but it is normally time consuming to achieve focus conditions. It is limited by multiple solutions and effects of higher order aberrations. Therefore, a combined method proposed in FANM is presented in this paper. FANM adopts the first order matrix method to achieve focus conditions and output currents of lenses for calculation of higher order aberration coefficients using the numerical ray tracing method.

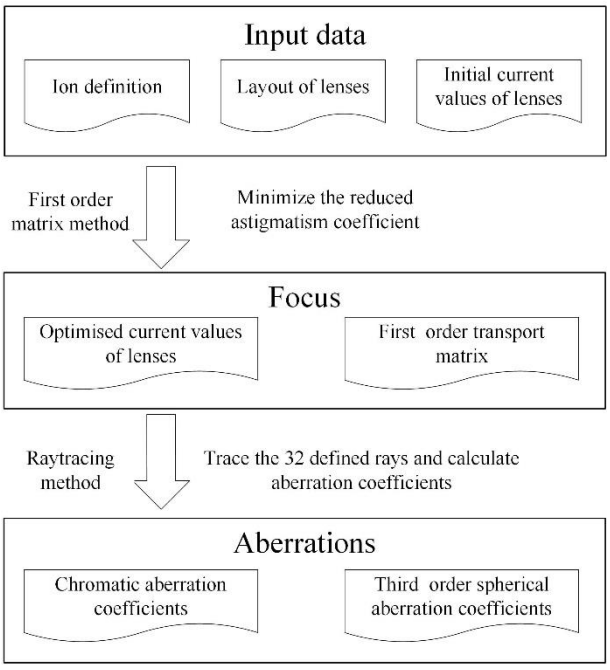

Fig. 1. The block diagram of FANM.

The block diagram of FANM is shown in Fig. 1. FANM includes three parts: input data, focus and aberrations. The first part is to define ion, layout of lenses and initial current values of lenses. The second part is to search for the excitations of in focus and output the optimized current values of the lenses as well as the first order transport matrix. The third part is to calculate higher order aberration coefficients using the optimized conditions.

(1) Input data

Input data of FANM are ion definition parameters, layout of lenses and initial current

values of lenses. As mentioned above, ion definition for beam optics design only needs magnetic rigidity of an ion. After user sets charge, kinetic energy and relative atomic mass of an ion, FANM converts those into magnetic rigidity. Kinetic energy and momentum of an ion are converted using relativistic formulas.

A layout of lenses includes geometrical length, spacing and magnetic gradient of lenses. Magnetic gradient of a lens is defined by its inner radius, current and number of turns of coils. The default setting of fringe fields of a lens in FANM is a rectangular model (hard-edge model) with the advantage of its simplicity and showing spherical aberrations of a lens system. It is worth noting that fringe fields of a lens bring extra spherical aberrations, which influence spherical aberrations of a focusing lens system. Spherical aberrations of a lens system can be compensated by shaping fringe fields of lenses. The Enge fringe field model may be more adequate to achieve better accuracy since it can fit experimentally determined field profiles more accurately [15]. Therefore, the Enge fringe field model is an optional choice in FANM to model fringe fields.

Initial current values are required by the default optimization algorithm (derivative-free method) in FANM. User needs some experience to set initial current values of lenses to obtain an optimized result with satisfactory performance. Normally there are multiple solutions to achieve focus conditions, possibly with quite different performance. The optional optimization algorithm (particle swarm optimization) in FANM requires setting the range of variables.

(2) Focus

FANM uses the first order matrix method to achieve focus conditions rapidly. Details of the first order matrix method can be found in [16], here is a brief description. In the first order matrix method, the state of an ion is written as a vector, and the ion transport through a drift or a quadrupole lens can be described with matrices. The transport matrix of a nuclear microprobe system can be built up by application of the matrix of each element in turn. The transport system is stigmatic with $< x|\theta >=< y|\varphi >= 0$ (i.e. focus conditions). When the reduced astigmatism coefficient ($\sqrt{< x|\theta >^2+< y|\varphi >^2}$) is close to zero, the transport system is in focus in FANM.

Current values of quadrupole lenses are adjusted by a numerical optimization routine to find the minimum of the reduced astigmatism coefficient. FANM offers two optional optimization algorithms (derivative-free method and particle swarm optimization) to solve it. Specifically, the fminsearch function and pso function in Matlab [26] are optional in FANM to achieve the minimization. After the optimization, the optimized currents of the lenses are used to produce the transport matrix of the system.

Note that, a focusing lens system normally has several local minimum conditions, resulting in multiple solutions. A higher excitation current usually produces a higher demagnification and aberrations. Some practical limiting factors will benefit from high demagnification, such as slits opening, stray AC magnetic field and vibration. Therefore, a high demagnification solution is normally a prioritized choice.

(3) Aberrations

FANM adopts a numerical ray tracing method to calculate higher order aberration coefficients, using the optimized currents of lenses from the first order matrix method. Details of the numerical ray tracing method can be found in [27]. In principle, the numerical ray tracing method can calculate aberration coefficients up to any order by changing the number of rays. However, the chromatic aberration and third order spherical aberration are major limitations in most cases. Therefore, FANM calculates the chromatic aberration coefficients and third order spherical aberration coefficients by tracing 32 defined rays.

The 32 defined rays and the aberration coefficients matrix of a focusing lens system in FANM are the same as those used in GEANT4-nanobeam [28]. In FANM, the Matlab function ode45 is used to track rays when propagating through a focusing lens system. The aberration coefficients (1×32) matrix is obtained by multiplying the inverse of a (32×32) matrix containing the power terms of the input parameters for each ray and a (32×1) matrix of image plane coordinates. Note that, the matrix inversion is only available for specific combination of rays.

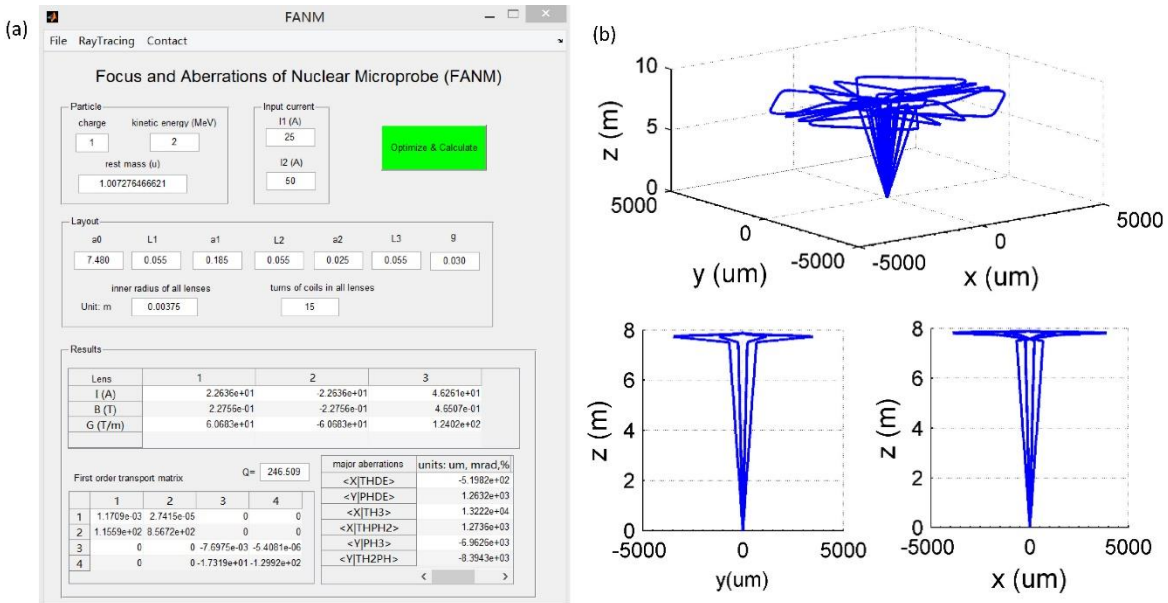

Fig. 2. FANM user interfaces. (a) Main interface. (b) Ray tracing graphs.

FANM user interfaces are shown in Fig. 2, including a main interface and ray tracing graphs. Ray tracing function for simulations is optional on the menu bar (Fig. 2(a)). Results tracing the 32 defined rays are shown in Fig. 2 (b), including xyz three-dimensional space, yz and xz two-dimensional space. The rays propagate along z-axis.

3. Comparisons with other software packages

Computational tools like TRANSPORT [29][30], Zgoubi [31][32], COSY INFINITY [33][34], Polymorphic Tracking Code (PTC) [35], Methodical Accelerator Design (MAD) [36][37], SixTRACK [38][39], IBSIMU [40], are widely used in the beam optics design of accelerators and beamlines. Based on the TRANSPORT version by K. L. Brown et al, PSI Graphic Transport Framework (TRANSPORT-PSI) [41] and PBO Lab TRANSPORT Application Module (TRANSPORT-PBO) [42] were developed respectively to have graph windows and more functions. In the nuclear microprobe community, three other software

packages are developed: Propagate Rays and Aberrations with Matrices (PRAM) [16], WinTRAX [27] and GEANT4-nanobeam [28]. To our best knowledge, six software packages (PRAM, TRANSPORT-PSI, TRANSPORT-PBO, WinTRAX, GEANT4-nanobeam and Zgoubi) are used in most of beam optics research in the nuclear microprobe community. Therefore, the six software packages are selected as a comparison with FANM.

Some studies presented a comparison of several packages of the six. Comparisons of PRAM, TRANSPORT and TRAX (superseded by WinTRAX) conclude an agreement within 2% in low order coefficients [16]. Our paper extends comparisons to high order coefficients. Comparisons of WinTRAX, GEANT4-nanobeam and Zgoubi based on the configuration of CENBG nanobeam show a remarkable agreement [27][28]. However, some discrepancies are discussed in our paper. A comparison between FANM and the six packages in details are shown in Table 1, Table 2 and Table 3. It is worth noting that GEANT4-nanobeam has a unique ability to simulate the ion-matter interaction. This advantage extends GEANT4-nanobeam to more applications, such as modeling slit scattering [43] and simulation of ion beam analysis [44]. Therefore, further development based on GEANT4-nanobeam codes is planned.

Basic information and major functions of the seven beam optics software (FANM, PRAM, TRANSPORT-PSI, TRANSPORT-PBO, WinTRAX, GEANT4-nanobeam and Zgoubi) for the design of a nuclear microprobe are summarized in Table 1. There are several methods to define a distribution of magnetic fields: (1) Use magnetic gradient of a lens; (2) Use pole field and inner radius of a lens; (3) Use number of turns of coils, coil current and inner radius of a lens. Besides, fringe field models are required. In FANM, the third method is selected to offer a reference for excitation currents in experiments. Meanwhile, pole field and magnetic gradient are also shown in FANM for convenience. As mentioned before, the rectangular model and the Enge fringe field are optional to model fringe fields in FANM. FANM uses the same figure of merit [23] as PRAM to give a rough indicator to system performance. This function saves time during a searching for high quality beam optics design. The ray tracing function is not available for PRAM, TRANSPORT-PSI and TRANSPORT-PBO. They need other tools (shown in Table 1) to trace rays. Most of the seven packages have a user friendly version on Windows platform, except GEANT4-nanobeam and Zgoubi. The GEANT4-nanobeam is hard to use since user should have knowledge of C++. FANM is very easy to use since only few input parameters are required. The download links of the seven software packages are shown in Table 1.

Accepted by Ultramicroscopy: https://doi.org/10.1016/j.ultramic.2020.113163

Table 1. Basic information and major functions of the seven beam optics software packages

Software	FANM	PRAM	TRANSPORT-PSI	TRANSPORT-PBO	WinTRAX	GEANT4-nanobeam	Zgoubi
Last update	2020	2016	2014	2020	2019	2019	2016
Ions	Yes	Yes	Yes	Yes	Yes	Yes	Yes
Quadrupole lens							
Coil current	Yes	Yes	No	No	Yes	No	No
Pole field	Yes	Yes	Yes	Yes	Yes	No	Yes
Magnetic gradient	Yes	No	No	Yes	No	Yes	No
Fringe field	Yes	Yes	Yes	Yes	Yes	Yes	Yes
Coefficients							
Demagnification	Yes	Yes	Yes	Yes	Yes	Yes	Yes
Chromatic aberration	Yes	Yes	Yes	Yes	Yes	Yes	Yes
Spherical aberration	Yes	Yes	No	Yes	Yes	Yes	Yes
Others							
Figure of merit (Q)	Yes	Yes	No	No	No	No	No
First order transport matrix	Yes	Yes	Yes	Yes	Yes	No	Yes
Ray tracing	Yes	+ OXTRACE	+ TURTLE	+ TURTLE	Yes	Yes	Yes
Platforms	Windows	Windows/Linux	Windows/Linux/ MacOS	Windows/Linux/ MacOS	Windows	Linux/Windows/ MacOS	Linux/Windows
Ease of use	Very easy	Normal	Normal	Easy	Easy	Hard	Normal
Pricing	Free	Free	Free	Charged	Free	Free	Free
Tutorial	Yes	Yes	Yes	Yes	Yes	Yes	Yes
Download link	[45]	[46]	[47]	[48]	[49]	[50]	[51]

The following comparisons of the seven beam optics software packages are based on the second generation proton beam writing beamline (2nd PBW) [52] in the Centre for Ion Beam Applications (CIBA), National University of Singapore. The layout of the 2nd PBW is shown in Fig. 3. Ions start from the object slits and end at the target. The +A–A+B configuration represents the system of three quadrupole lenses arranged converging, diverging and converging. Meanwhile, the first and second quadrupole lens are coupled. The structure of the three quadruple lenses is the same, with a length of 55 mm, an inner radius of 3.75 mm, and 15 turns of coils. The symbol "a" stand for a drift, "g" is a special drift named working distance, and "L" stand for geometrical length of a lens. The total length of the 2nd PBW system is 7885 mm. Because most of the seven beam optics software can only deal with straight beamline, the switching magnet between the object slits and collimator in the 2nd PBW system is not shown and simply regarded as a drift.

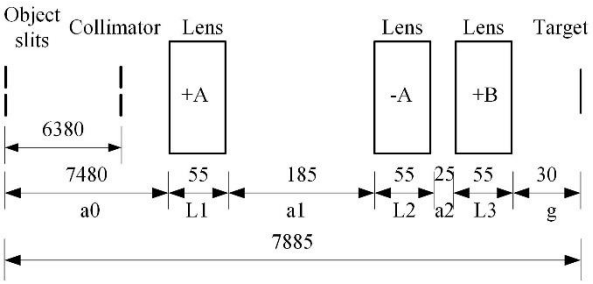

Fig. 3. Layout of the second generation proton beam writing beamline (2nd PBW) in Singapore (unit: mm).

As shown in Table 2, there are three methods to define an ion in beam optics designs: (1) FANM, PRAM, TRANSPORT-PBO, WinTRAX and GEANT4-nanobeam use the same ion definition method with three input parameters (kinetic energy, rest mass and charge number). (2) TRANSPORT-PSI uses two input parameters (momentum and charge number) to define an ion. (3) Zgoubi uses one input parameter (magnetic rigidity) to define an ion. The three methods define equivalently an ion in a magnetic field. In Table 2, GEANT4-nanobeam and Zgoubi adopt the pole fields calculated by FANM. The pole fields optimized by FANM, PRAM, TRANSPORT-PSI, TRANSPORT-PBO and WinTRAX show a good agreement. The demagnification calculated by the seven beam optics software packages also show a good agreement.

Note that, fundamental physical constants used in the seven packages are not all the same. For example, in GEANT4-nanobeam, the rest mass of proton is defined as 938.272013 MeV not 938.27208816 MeV (2018 CODATA recommended values), and the elementary charge is defined as $1.602176487e^{-19}$ C not $1.602176634e^{-19}$ C (2018 CODATA recommended values). FANM utilizes the 2018 CODATA recommended values of the fundamental physical constants from NIST [53]. The conversion result of momentum and magnetic rigidity is listed as a reference using FANM (not shown in the user interface). Another difference among the seven packages is their calculation accuracy, most of them only use 8 significant digits or less accuracy. PRAM employs double precision arithmetic. FANM accepts 16 significant digits for input parameters and stores numeric variables as 64-bit (8-byte) double-precision floating-point values to reduce calculation errors. These two

differences result in a slight discrepancy of the optimized pole field. The slight discrepancy may not influence the calculation of aberrations, but may be an issue to trace an ion on nanoscale.

Results calculated by the seven beam optics software packages using the rectangular model are shown in Table 2. After the focusing lens system is optimized to be in focus, the astigmatism coefficients (focus conditions) are extremely close to zero except WinTRAX. This validates the shortage of ray tracing method, its optimization processing influenced by high order aberrations makes the optimization procedure time consuming and not easy to obtain good focus conditions. The optimized pole fields by WinTRAX are slight different compared to other software packages, resulting in slight different demagnifications. GEANT4-nanobeam and Zgoubi using the optimized pole fields from FANM achieve smaller astigmatism coefficients than WinTRAX. This confirms the advantage of the combined method to make a focusing lens system in focus.

As shown in Table 2, the chromatic coefficients calculated by the seven beam optics software packages agree well within 1% except Zgoubi, which are 50% smaller than the other packages. This odd result may be caused by the wrong definition of chromatic coefficients: Zgoubi may use energy spread in its codes, not momentum spread as claimed in its manual [54]. The authors of Zgoubi discussed the difference of the two definitions in their early publication [55], the two definitions of chromatic coefficients are converted by a factor of about 2. Therefore, the error in chromatic coefficients in Zgoubi may ascribe to its upgrade. The other six software packages use momentum spread to define chromatic coefficients, which can be directly applied to both non-relativity and relativity situations.

Accepted by Ultramicroscopy: https://doi.org/10.1016/j.ultramic.2020.113163

Table 2. Ion definition methods and results calculated by the seven beam optics software packages using the rectangular model

	Combined method	Matrix method			Numerical ray tracing method		
	FANM	PRAM	TRANSPORT-PSI	TRANSPORT-PBO	WinTRAX	GEANT4-nanobeam	Zgoubi
Ion							
Kinetic energy (MeV)	2	2	-	2	2	2	-
Rest mass in u or MeV	1.007276466621 u	1.007276 u	-	1.007276 u	1.007276 u	938.272013 MeV	-
Momentum (MeV/c)	(61.29509240261)	-	61.29509	-	-	-	-
Charge number	1	1	1	1	1	1	1
Magnetic rigidity (Tm)	(0.2044584203736)	-	-	-	-	-	0.204458
Quadrupole lens							
Pole field A(T)	0.2275613	0.227562	0.227561	0.2275613	0.2275586	0.2275613	0.227561
Pole field B(T)	0.4650671	0.465069	0.465067	0.4650669	0.4650491	0.4650671	0.465067
Focus conditions							
$\langle x\|\theta\rangle$ (μm*mrad^{-1})	2.7415E–05	5.447E–08	0.0000	0.00001	–2.1262	–3.2365E–02	1.1522E–04
$\langle y\|\varphi\rangle$ (μm*mrad^{-1})	–5.4081E–06	1.384E–07	0.0000	0.00001	0.67418	2.0720E–02	3.3314E–05
Demagnification							
D_x, $\langle\theta\|\theta\rangle$	856.72	856.72	856.72	856.72	856.67	856.72	856.72
D_y, $\langle\varphi\|\varphi\rangle$	–129.92	–129.92	–129.92	–129.92	–129.92	–129.92	–129.92
Chromatic coefficients							
$\langle x\|\theta\delta\rangle$ (μm*mrad^{-1}%$^{-1}$)	–519.82	–516.35	–519.8	–519.8	–520.33	–520.37	–260
$\langle y\|\varphi\delta\rangle$ (μm*mrad^{-1}%$^{-1}$)	1263.2	1255.4	1263	1263	1264.5	1264.5	632
Spherical coefficients							
$\langle x\|\theta^3\rangle$ (μm*mrad^{-3})	13222	28906	-	24040	13154	13222	13154
$\langle x\|\theta\varphi^2\rangle$ (μm*mrad^{-3})	1273.6	4817.4	-	10850	1269.5	1273.6	-
$\langle y\|\varphi^3\rangle$ (μm*mrad^{-3})	–6962.6	–27165	-	–24510	–6951.5	–6962.5	–6951.8
$\langle y\|\theta^2\varphi\rangle$ (μm*mrad^{-3})	–8394.3	–31767	-	–71560	–8371.1	–8394.2	-
Figure of merit (Q)	246.51	120.65	-	-	-	-	-

Accepted by Ultramicroscopy: https://doi.org/10.1016/j.ultramic.2020.113163

The spherical coefficients calculated by the seven beam optics software packages are shown in Table 2. Obviously, the spherical coefficients by the matrix method and numerical ray tracing method are quite different. The discrepancies of spherical coefficients are caused by their dealing with fringe fields. PRAM and TRANSPORT-PBO are not using rectangular model when calculate spherical coefficients, they actually use a modified rectangular model in their codes. Note that, a modified rectangular model is limited to certain structure of quadrupole lens. PRAM and TRANSPORT-PBO are different in cross-terms of spherical coefficients, confirming they are using different modified rectangular model in their codes. TRANSPORT-PSI cannot give spherical coefficients since it is only up to second order matrix. The spherical coefficients by FANM, WinTRAX, GEANT4-nanobeam and Zgoubi agree well within 1%. It is not surprising that FANM, WinTRAX and GEANT4-nanobeam can agree extremely well in aberration calculation since they are using the same principle of numerical ray tracing method. The definition of figure of merit is mentioned above. FANM and PRAM show the figure of merit directly, other software packages have to calculate it by hand using the values of demagnification and spherical aberration coefficients.

Table 3. Results calculated by FANM, WinTRAX, PRAM and TRANSPORT-PBO using other magnetic field models

	FANM*	WinTRAX*	PRAM**	TRANSPORT-PBO**
Quadrupole lens				
Magnetic field model	Enge fringe field model	Enge fringe field model	modified rectangular model	modified rectangular model
Pole field A(T)	0.2033270	0.2033272	0.216867	0.216866
Pole field B(T)	0.4172323	0.4172594	0.444021	0.444019
Focus conditions				
$\langle x\|\theta\rangle$ (μm*mrad^{-1})	–7.6350E–06	4.2131	6.950E–05	–0.00001
$\langle y\|\varphi\rangle$ (μm*mrad^{-1})	2.7931E–05	0.26298	1.189E–04	0.00000
Demagnification				
D_x, $\langle\theta\|\theta\rangle$	907.30	907.36	874.30	874.30
D_y, $\langle\varphi\|\varphi\rangle$	–133.78	–133.77	–131.19	–131.19
Chromatic coefficients				
$\langle x\|\theta\delta\rangle$ (μm*mrad^{-1}%$^{-1}$)	–524.85	–525.51	–517.77	–521.3
$\langle y\|\varphi\delta\rangle$ (μm*mrad^{-1}%$^{-1}$)	1409.5	1411.1	1304.1	1312
Spherical coefficients				
$\langle x\|\theta^3\rangle$ (μm*mrad^{-3})	23844	23657	28895	23850
$\langle x\|\theta\varphi^2\rangle$ (μm*mrad^{-3})	12385	12239	4738.6	11380
$\langle y\|\varphi^3\rangle$ (μm*mrad^{-3})	–27744	–27684	–28670	–25670
$\langle y\|\theta^2\varphi\rangle$ (μm*mrad^{-3})	–83752	–83187	–31580	–75870
Figure of merit (Q)	139.31	-	122.13	-

*The coefficients of Enge fringe filed model are from the OM52 in WinTRAX example (z0=0.023, z1=0.025, c0=–8, c1=3, c2=c3=c4=0).

**In the modified rectangular model, L=l+1.1r was assumed to give the effective physical length of a lens where l is the geometrical length, r is the inner radius of a lens.

As a comparison with the rectangular model, the calculated results using other magnetic field models are presented in Table 3. It can be seen that the pole fields, demagnification, chromatic and spherical coefficients by FANM agree with WinTRAX. The focus conditions optimized by FANM (particle swarm optimization method) are much closer to zero compared with WinTRAX. This validates an enhancement of optimization algorithm in FANM. Obviously, the calculated results by FANM are different with PRAM and TRANSPORT-PBO because of the difference to deal with fringe fields. The effective physical length is not the same, changes the values of pole fields and demagnifications. It is interesting that the chromatic and spherical coefficients by FANM agree with TRANSPORT-PBO. Note that, calculated spherical coefficients depend on the quality of modelling fringe fields [17] [56].

As expected, the spherical coefficients calculated with fringe fields (i.e. Enge fringe field model in Table 3) are quite different compared to the ones calculated without fringe fields (i.e. rectangular model in Table 2). The results of pole fields and demagnifications are also affected by fringe fields since the effective length of a lens changes. Therefore, a suitable magnetic field model is required to model real nuclear microprobes. FANM offers this choice using Enge fringe field model.

4. Comparisons with experimental results

In this paper, two factors from experimental results in the 2nd PBW system are chosen to validate FANM: demagnification and excitation current. A previous experimental study demonstrated the 2nd PBW system has a demagnification of about 857×130 [52]. This validates the demagnification (857×130) calculated by FANM. Note that, the accuracy of object opening and spot size measurement limit the reproduce. A compact electronic scanner in front of the focusing lens system has a similar structure in xoz and yoz plane. Therefore, the ratio of scanner voltage in xoz and yoz plane may equal to the ratio of demagnification in xoz and yoz plane when keep the same scan size in xoz and yoz plane. The scanner voltage is measured using an oscilloscope (TEKTRONIX-MDO3024, 8 bits vertical resolution). The scan size is calibrated by moving a piezoelectric XYZ positioning stage (PI N-310K059, resolution < 10 nm) with 5 micron and scanning a grid with a spot size of less than 100 nm. Using this method, the experimental uncertainty of the ratio of demagnification should be less than 5%. We measured the scanner voltages using 1 MeV H_2^+, 1.5 MeV H_2^+ and 2 MeV H_2^+ respectively, confirming the ratio of demagnification in xoz and yoz plane is about 6. This also validates the ratio of demagnification (6.6) calculated by FANM.

Excitation currents of quadrupole lenses are relatively easy to obtain. However, the real magnetic field of a quadrupole lens cannot simply described by an ideal model (using number of turns of coils, coil current and inner radius of a lens). Fortunately, the commercial quadrupole lenses used in the 2nd PBW system has a good linear relationship between pole field and excitation current. Therefore, we design a method using the ratio of excitation currents to validate FANM.

Here is a brief description of the experiments in the 2nd PBW system: six ion beams (1 MeV proton, 1.5 MeV proton, 2 MeV proton, 1 MeV H_2^+, 1.5 MeV H_2^+ and 2 MeV H_2^+) were respectively focused into a spot size of sub-100 nm (assuming the lens system is in focus),

and the excitation currents of the quadrupole lenses were recorded in each cases. The results are shown in Fig. 4. The quadrupole lens power supple has a stability of 2 ppm [52]. However, we only search for a minimum spot size (<100 nm) by tuning the lens power supply with a step of 0.01 A in these experiments. Thus the experimental uncertainty of the excitation currents of the quadrupole lenses is less than 0.02 A (i.e. less than 0.1%) in Fig. 4.

Obviously, 2 MeV proton and 1 MeV H_2^+ have a similar magnetic rigidity (0.204 Tm), thus these two measurements overlap in the Fig.4. As expected, there are systematic discrepancies between the ideal excitation current values calculated by FANM and the experimental values, while the ratio of excitation currents calculated by FANM agree with experimental values. The discrepancies could be explained that the practical quadrupole lens does not offer an ideal excitation curve due to the following reason: The practical pole shape is not constructed with an ideal pole shape (infinite hyperboloid), and the practical geometrical structure of the quadrupole lenses affects quadrupole magnet excitation curve.

As shown in Fig. 4, a linear relationship between ion magnetic rigidity and excitation currents is observed in experiments, matching the prediction by FANM. This is benefit from the 2nd PBW system use the same quadrupole lenses purchased from a company and those quadrupole lenses are not obviously suffer from saturation of the magnetic field with a lens current less than 70 A. Users can easily find a correction coefficient for excitation currents calculated by FANM to match experimental results. In Fig. 4, the correction coefficient for excitation currents calculated by FANM is about 1.1. Therefore, results by FANM can be used as a reference for experimental settings.

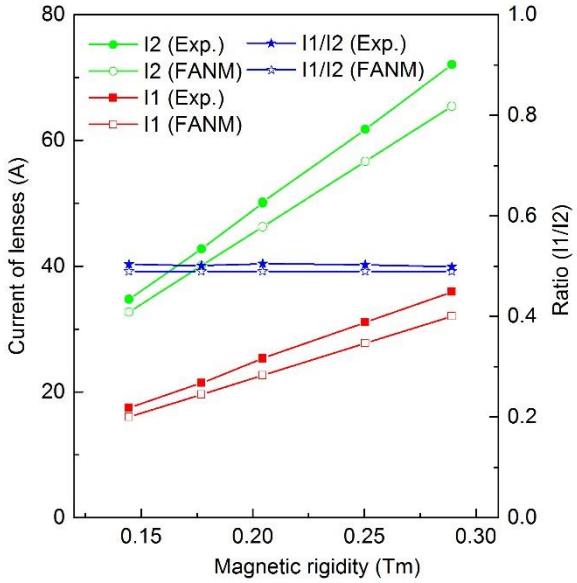

Fig. 4. Comparisons of excitation currents of quadrupole lenses calculated by FANM and recorded from experiments in the 2nd PBW system. The lines are guide for the eyes. See text for details.

5. Conclusions

FANM is a new tool to search for high quality beam optics designs for a nuclear microprobe. It runs in Windows system on personal laptop within seconds and only requires a

few input parameters. A combined method proposed in FANM achieves a balance between speed of focusing and accuracy of high order aberrations. The remarkable agreement with WinTRAX and Geant4-nanobeam validates the accuracy of FANM. FANM shows an enhancement of optimization ability by using two optional optimization algorithms (derivative-free method and particle swarm optimization). Numeric variables stored as 64-bit (8-byte) double-precision floating-point values and updated fundamental physical constants make FANM with lower calculation errors compared with the other six software packages. Comparisons with experimental results confirm FANM can be used as a reference for experimental settings.

Acknowledgements

The author Yanxin Dou acknowledges the discussions with Prof. David Norman Jamieson (University of Melbourne) comparing the six beam optics software using the nuclear microprobe in Melbourne. The authors acknowledge funding support from the support from the United States Air Force (FA9550-18-1-0110 and FA9550-20-1-0249), as well as the support from Singapore's National Research Foundation (NRF) Competitive Research Programme (CRP) (Award No. NRF-CRP13-2014-04).

References

[1] Mayer, James W., and E. Rimini. Ion beam handbook for material analysis. Elsevier, 2012.

[2] Chu, W. K., et al. "Principles and applications of ion beam techniques for the analysis of solids and thin films." Thin Solid Films 17.1 (1973): 1-41.

[3] Schaffer, Miroslava, et al. "Automated three-dimensional X-ray analysis using a dual-beam FIB." Ultramicroscopy 107.8 (2007): 587-597.

[4] Lee, Eal H. "Ion-beam modification of polymeric materials–fundamental principles and applications." Nuclear Instruments and Methods in Physics Research Section B: Beam Interactions with Materials and Atoms 151.1-4 (1999): 29-41.

[5] Popok, Vladimir N. "Ion implantation of polymers: formation of nanoparticulate materials." Rev. Adv. Mater. Sci 30.1 (2012): 1-26.

[6] Feng, Huiyun, Zengliang Yu, and Paul K. Chu. "Ion implantation of organisms." Materials Science and Engineering: R: Reports 54.3-4 (2006): 49-120.

[7] Van Kan, Jeroen A., Andrew A. Bettiol, and Frank Watt. "Proton beam writing of three-dimensional nanostructures in hydrogen silsesquioxane." Nano letters 6.3 (2006): 579-582.

[8] Watt, F., et al. "Ion beam lithography and nanofabrication: a review." International Journal of Nanoscience 4.03 (2005): 269-286.

[9] Larson, D. J., et al. "Field-ion specimen preparation using focused ion-beam milling." Ultramicroscopy 79.1-4 (1999): 287-293.

[10] McCaffrey, J. P., M. W. Phaneuf, and L. D. Madsen. "Surface damage formation during ion-beam thinning of samples for transmission electron microscopy." Ultramicroscopy 87.3 (2001): 97-104.

[11] Krasheninnikov, A. V., and Kai Nordlund. "Ion and electron irradiation-induced effects

in nanostructured materials." Journal of applied physics 107.7 (2010): 3.
[12] Ishikawa, Satoru, et al. "Ion-beam irradiation, gene identification, and marker-assisted breeding in the development of low-cadmium rice." Proceedings of the National Academy of Sciences 109.47 (2012): 19166-19171.
[13] Kim, Suhan, et al. "Minimization of focused ion beam damage in nanostructured polymer thin films." Ultramicroscopy 111.3 (2011): 191-199.
[14] https://nucleus.iaea.org/sites/accelerators/Pages/default.aspx
[15] Grime, Geoff W., and Frank Watt. "Beam optics of quadrupole probe-forming systems." Beam Opt of Quadrupole Probe-Form Syst (1984).
[16] Breese, Mark BH, David N. Jamieson, and Philip JC King. "Materials analysis using a nuclear microprobe." John! Wiley & Sons Ltd, Journals, Baffins Lane, Chichester, Sussex PO 19 1 UD, UK, 1996. 428 (1996).
[17] Jamieson, David N. "New generation nuclear microprobe systems." Nuclear Instruments and Methods in Physics Research Section B: Beam Interactions with Materials and Atoms 181.1-4 (2001): 1-11.
[18] Szymanski, Roland, and David N. Jamieson. "Ion source brightness and nuclear microprobe applications." Nuclear Instruments and Methods in Physics Research Section B: Beam Interactions with Materials and Atoms 130.1-4 (1997): 80-85.
[19] Miroshnichenko, V. I., et al. "Possibility to increase RF ion source brightness for nuclear microprobe applications." Nuclear Instruments and Methods in Physics Research Section B: Beam Interactions with Materials and Atoms 201.4 (2003): 630-636.
[20] Matsuyama, S., et al. "Upgrading of the 4.5 MV Dynamitron accelerator at Tohoku University for microbeam and nanobeam applications." Nuclear Instruments and Methods in Physics Research Section B: Beam Interactions with Materials and Atoms 267.12-13 (2009): 2060-2064.
[21] Van Kouwen, Leon, and Pieter Kruit. "Brightness measurements of the nano-aperture ion source." Journal of Vacuum Science & Technology B, Nanotechnology and Microelectronics: Materials, Processing, Measurement, and Phenomena 36.6 (2018): 06J901.
[22] Van Kan, Jeroen A., et al. "Considerations for the nano aperture ion source: Geometrical design and electrical control." Review of Scientific Instruments 91.1 (2020): 013310.
[23] Ryan, Chris G., and David N. Jamieson. "A high performance quadrupole quintuplet lens system for the CSIRO–GEMOC nuclear microprobe." Nuclear Instruments and Methods in Physics Research Section B: Beam Interactions with Materials and Atoms 158.1-4 (1999): 97-106.
[24] Van Kan, J. A., P. Malar, and Armin Baysic de Vera. "The second generation Singapore high resolution proton beam writing facility." Review of scientific instruments 83.2 (2012): 02B902.
[25] Qureshi, Sarfraz, et al. "Quadrupole lens alignment with improved STIM and secondary electron imaging for Proton Beam Writing." Nuclear Instruments and Methods in Physics Research Section B: Beam Interactions with Materials and Atoms 404 (2017): 74-80.
[26] Higham, Desmond J., and Nicholas J. Higham. MATLAB guide. Society for Industrial and Applied Mathematics, 2016.

[27] Grime, G. W. "WinTRAX: A raytracing software package for the design of multipole focusing systems." Nuclear Instruments and Methods in Physics Research Section B: Beam Interactions with Materials and Atoms 306 (2013): 76-80.
[28] Incerti, S., et al. "A comparison of ray-tracing software for the design of quadrupole microbeam systems." Nuclear Instruments and Methods in Physics Research Section B: Beam Interactions with Materials and Atoms 231.1-4 (2005): 76-85.
[29] Brown, Karl L., et al. TRANSPORT-A computer program for designing charged particle beam transport systems. No. CERN--80-04. European Organization for Nuclear Research, 1980.
[30] Brown, Karl. Third-order TRANSPORT with MAD input: A computer program for designing charged particle beam transport systems. No. SLAC-R-530. Stanford Linear Accelerator Center, Menlo Park, CA (US), 1998.
[31] Méot, François. "The ray-tracing code Zgoubi." Nuclear Instruments and Methods in Physics Research Section A: Accelerators, Spectrometers, Detectors and Associated Equipment 427.1-2 (1999): 353-356.
[32] Méot, F. "The ray-tracing code Zgoubi–Status." Nuclear Instruments and Methods in Physics Research Section A: Accelerators, Spectrometers, Detectors and Associated Equipment 767 (2014): 112-125.
[33] Berz, Martin. "Computational aspects of optics design and simulation: COSY INFINITY." Nuclear Instruments and Methods in Physics Research Section A: Accelerators, Spectrometers, Detectors and Associated Equipment 298.1-3 (1990): 473-479.
[34] Makino, Kyoko, and Martin Berz. "Cosy infinity version 9." Nuclear Instruments and Methods in Physics Research Section A: Accelerators, Spectrometers, Detectors and Associated Equipment 558.1 (2006): 346-350.
[35] Forest, Etienne, Frank Schmidt, and Eric McIntosh. "Introduction to the polymorphic tracking code." KEK report 3 (2002): 2002.
[36] Grote, Hans, et al. "The MAD program." Proceedings of the 1989 IEEE Particle Accelerator Conference,.'Accelerator Science and Technology. IEEE, 1989.
[37] Grote, Hans, and F. Christoph Iselin. The MAD program (methodical accelerator design): version 8.10; user's reference manual. No. CERN-SL-90-13-AP-rev-3. CM-P00049316, 1993.
[38] Schmidt, Frank. SIXTRACK: version 1, single particle tracking code treating transverse motion with synchrotron oscillations in a symplectic manner. No. CERN-SPS-88-51-AMS-rev. CM-P00049314, 1990.
[39] Robert-Demolaize, Guillaume, et al. "A new version of SixTrack with collimation and aperture interface." Proceedings of the 2005 Particle Accelerator Conference. IEEE, 2005.
[40] Kalvas, Taneli, et al. "IBSIMU: A three-dimensional simulation software for charged particle optics." Review of Scientific Instruments 81.2 (2010): 02B703.
[41] PSI Graphic Transport Framework by U. Rohrer based on a CERN-SLAC-FERMILAB version by K.L. Brown et al.
[42] Gillespie, George H., and Barrey W. Hill. "Particle optics and accelerator modeling software for industrial and laboratory beamline design." Nuclear Instruments and Methods in

Physics Research Section B: Beam Interactions with Materials and Atoms 139.1-4 (1998): 476-480.
[43] Dou, Yanxin, et al. "GEANT4 models for the secondary radiation flux in the collimation system of a 300 MeV proton microbeam." Physica Medica 32.12 (2016): 1841-1845.
[44] Pia, Maria Grazia, et al. "PIXE simulation with Geant4." IEEE transactions on nuclear science 56.6 (2009): 3614-3649.
[45] https://github.com/CHNDOU/FANM
[46] https://www.ph.unimelb.edu.au/~dnj/research/pram/pramdist.htm
[47] http://aea.web.psi.ch/Urs_Rohrer/MyFtp/
[48] http://www.ghga.com/accelsoft/catalog.html
[49] http://www.microbeams.co.uk/download.html
[50] https://geant4.web.cern.ch/support/download
[51] https://sourceforge.net/projects/zgoubi/
[52] Yao, Y., and J. A. Van Kan. "Automatic beam focusing in the 2nd generation PBW line at sub-10 nm line resolution." Nuclear Instruments and Methods in Physics Research Section B: Beam Interactions with Materials and Atoms 348 (2015): 203-208.
[53] https://www.nist.gov/pml/fundamental-physical-constants
[54] Méot, F. Zgoubi users guide. No. BNL-98726-2012-IR. BROOKHAVEN NATIONAL LABORATORY (BNL), 2012.
[55] Méot, F. "Generalization of the Zgoubi method for ray-tracing to include electric fields." Nuclear Instruments and Methods in Physics Research Section A: Accelerators, Spectrometers, Detectors and Associated Equipment 340.3 (1994): 594-604.
[56] Dou, Yanxin, et al. "Investigation of intrinsic aberrations introduced by the fringing field in the proposed 300 MeV proton microprobe in Harbin." Nuclear Instruments and Methods in Physics Research Section B: Beam Interactions with Materials and Atoms 450 (2019): 380-384.